

Study on Flow Fields in Variable Area Nozzles for Radial Turbines

TAMAKI Hideaki : Doctor of Engineering, P. E. Jp, Manager, Turbo Machinery Department, Product Development Center, Corporate Research & Development
UNNO Masaru : Manager, Turbo Machinery Department, Product Development Center, Corporate Research & Development
IWAKAMI Akira : Manager, Development Department, Vehicular Turbocharger Operations
ISHII Shinnosuke : Fuji Heavy Industries Ltd.

The flow behind the variable area nozzle for radial turbines was measured with a 3-hole yaw probe and calculated with CFD. Two nozzle throat-areas were investigated, the smallest and the largest openings for the variable nozzle. Test results agreed with the calculated results qualitatively. The leakage flow through the tip clearance of the nozzle vane significantly affected the flow field downstream of the nozzle vane with the smallest opening. However, the effect on leakage flow on the flow field downstream of the nozzle vane was very weak with the largest opening, so significantly different flow fields were observed.

1. Introduction

Turbochargers supply compressed air to engines utilizing the exhaust energy of the engines. The turbine, driven by the energy from the exhaust gas, rotates the compressor, which charges the compressed gas into the engine. The more air is supplied to the engine, the more fuel can be injected into the engine and the engine output can be increased. With a diesel engine, increasing the air-fuel ratio improves the combustion, and therefore, largely reduces smoke in the exhaust gas and also reduces the specific fuel consumption. For this reason, the installation of the turbocharger for a diesel engine is now indispensable. A turbocharger equipped with a variable area nozzle system, a pivoting nozzle vane moved with an actuator, can change its nozzle throat area to meet the engine operation from idling to rated speed and is especially suited to realizing optimal turbine output for the different engine operating points.

Several design and performance predicting methods of the variable area nozzle for radial turbines have been reported. Meitner et al. proposed performance predicting methods of variable area nozzle, but they have not been verified through experiments.⁽¹⁾ Many researches were based on the stage performance of turbines and a few included measurement and analysis results of detailed internal flow.⁽²⁾⁻⁽⁴⁾ Hayami et al.⁽⁵⁾, Senoo et al.⁽⁶⁾, and Hyun et al.⁽⁷⁾ measured the flow field at the nozzle outlet in detail using the nozzle setting angle and clearance as parameters. However, the range of the nozzle setting angle (movable angle) for present turbochargers is much larger than that of their studies. Therefore it is necessary

to understand the flow field at the nozzle outlet in a wider range of the nozzle setting angle to design turbochargers with variable area nozzles.

In this research, therefore, such nozzle setting angles as to sufficiently include the working range of the variable area nozzle of the present turbochargers were determined and flow analysis and flow measurement were conducted at the minimum opening (throat area : small, setting angle : large when measured from the radial direction, hereinafter called the smallest opening) and maximum opening (throat area : large, setting angle : small, hereinafter called the largest opening). Especially the total pressure and flow angle distribution on the nozzle downstream section to greatly influence the performance of the turbine impeller were investigated.

2. Test equipment and test/calculation methods

Figure 1 shows the cross section of the test equipment. The flow passing through the turbine scroll is turned and runs into the nozzle. The flow angle at the scroll outlet was designed at 67.5° . The flow coming out of the nozzle is turned in the axial direction and discharged into the atmosphere. The flow field at the nozzle downstream portion was measured with a 3-hole yaw probe. The measurement position was located 0.5% downstream of the impeller radius from the turbine impeller inlet. The yaw probe could be moved in the nozzle circumferential direction with a precision slider support. The measurement was made at 7 to 9 points in the span direction (nozzle height direction, between the hub and shroud) and at 30 points, 2 degrees each, in the circumferential direction.

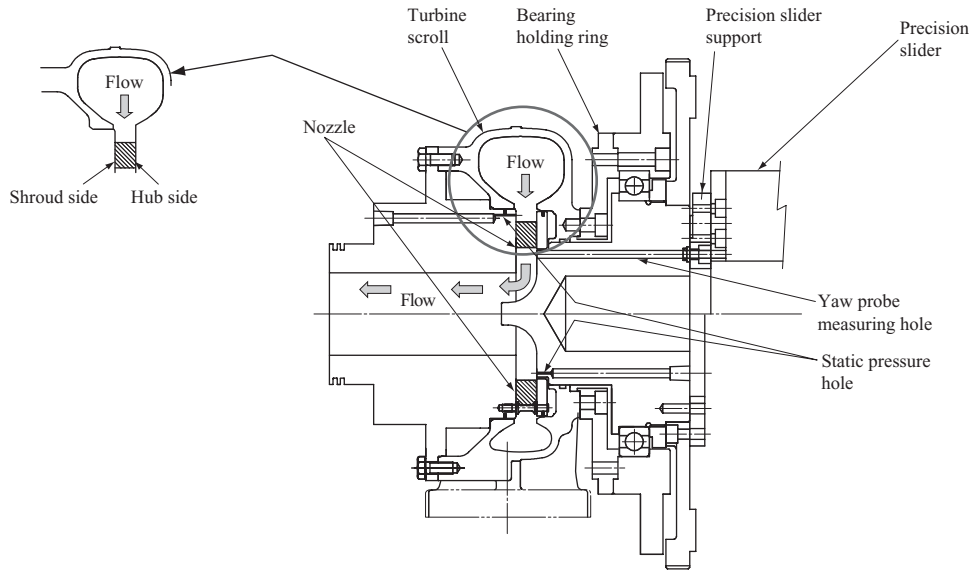


Fig. 1 Test rig

Figure 2 shows the shape of the nozzle cascade, and Table 1 shows representative dimensions. The throat width is a relative value with the largest opening as 1.0, and the measuring position for the nozzle outlet diameter is shown in the ratio to the diameter of the nozzle rotation center, the position of the pivot. In the test, non-rotational flow channel was used in place of the turbine impeller,

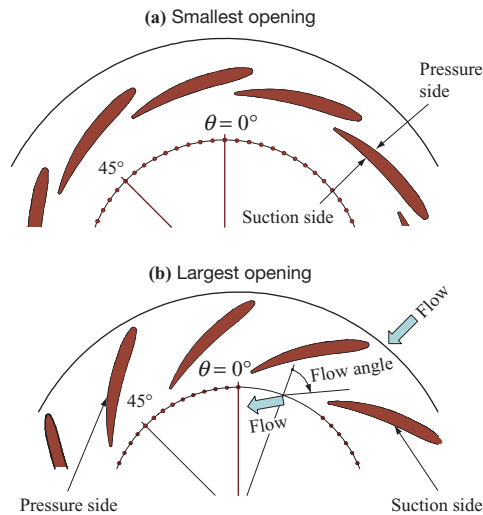


Fig. 2 Tested nozzles

Table 1 Nozzle main dimensions

Item	Inlet angle (degree)	Outlet angle (degree)	Nozzle vane height (mm)	Nozzle clearance (mm)	Throat width (-)	Position of nozzle trailing edge (-)	Measuring position (-)
Smallest opening	72.0	85.0	12.75	0.75	0.27	0.94	0.71
			13.50	0.0			
Largest opening	51.0	65.0	12.75	0.75	1.0	0.79	
			13.50	0.0			

and so it was difficult to determine if the nozzle test conditions corresponded to the operating points of the turbine. In understanding the nozzle internal flow pattern, however, the effect of the nozzle test conditions would not be significant. Table 2 shows the test conditions and calculation points. To check the effect of the clearance, the nozzle vanes with clearance and without clearance on the shroud side were used. In this research, the value of clearance was made 2.5 times that of the normal variable nozzle to clarify the effect of the clearance. In this paper, the pressure side and suction side are defined as shown in Fig. 2.

Figure 3 shows the computational grid. The calculation was made on the nozzle with clearance. For the vane portion, H-H type structural grids were arranged at 69 points in the span direction (including 20 points within the clearance), 57 points in the circumferential direction, and 69 points in the flow direction (233 points in total). For the calculation the code developed by IHI was applied. For the convective term, Chakravarthy-Osher TVD scheme was used, and for the turbulence, the Spalart-Allmaras model was used. As boundary conditions, total pressure, total temperature, and flow angle were fixed at the inlet boundary. The test value for the total temperature and the scroll outlet flow angle (design value) for the flow angle were used at the inlet boundary. At the outlet boundary, the static pressure was fixed to the atmospheric pressure, and the periodic boundary condition was used. The inlet total pressure was adjusted so that the static pressure ratio before and after the nozzle almost equaled the test value.

3. Test and calculation results

Figures 4 and 5 show calculation results of the smallest and largest openings of the nozzle, and Fig. 6 shows the results of oil flow visualization. The Mach number

Table 2 Test conditions and CFD results

Item	Nozzle vane height (mm)	Clearance (mm)	Test conditions		CFD results	
			$G\sqrt{T_0}/P_0$ $kg\sqrt{K}Pa^{-1}s^{-1} \times 10^{-4}$	P_{LE}/P_{TE} (-)	$G\sqrt{T_0}/P_0$ $kg\sqrt{K}Pa^{-1}s^{-1} \times 10^{-4}$	P_{LE}/P_{TE} (-)
Smallest opening	12.75	0.75	1.79	1.30	1.77	1.30
	13.50	0.0	1.28	1.30	1.33	1.32
Largest opening	12.75	0.75	4.12	1.07	4.20	1.06
	13.50	0.0	4.31	1.07	4.22	1.05

(Note) G : Flow (kg/s) P_{LE} : Static pressure at nozzle inlet
 T_0 : Inlet total temperature (K) P_{TE} : Static pressure at nozzle outlet
 P_0 : Inlet total pressure (Pa)

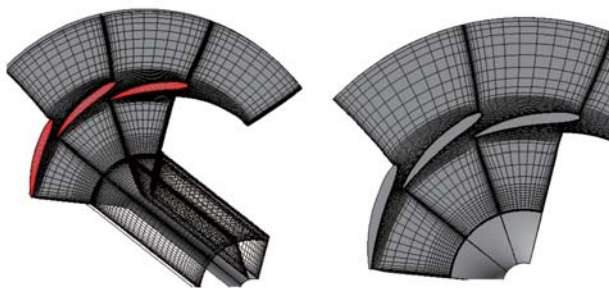


Fig. 3 Computational grid

distribution is that of the mid-span portion. The static pressure distribution on the blade shows the values of the mid-span and is made dimensionless at the scroll inlet total pressure.

In case of the smallest opening (**Fig. 4**), the flow has a positive incidence against the nozzle, and the pressure on the pressure side is higher than that on the suction side. At the overlap portion of the pressure side and suction side, a passage similar to a rectangle channel is formed, and in case of the smallest opening, the length of this passage is short. For this reason, the flow velocity on the pressure

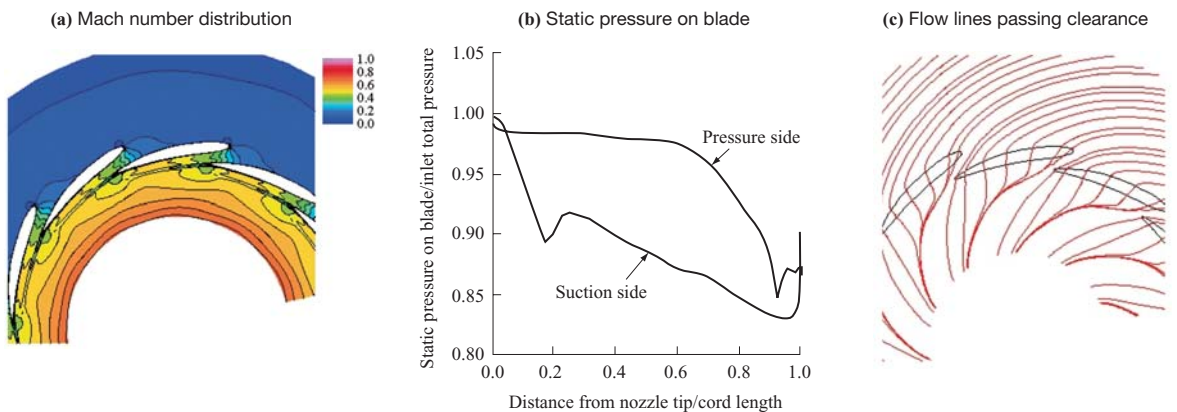


Fig. 4 Calculated result (Smallest opening)

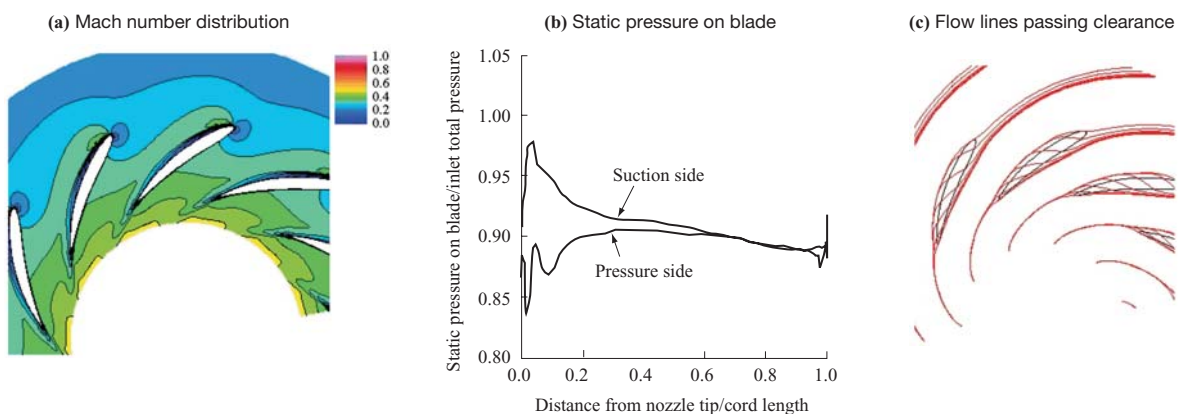


Fig. 5 Calculated result (Largest opening)

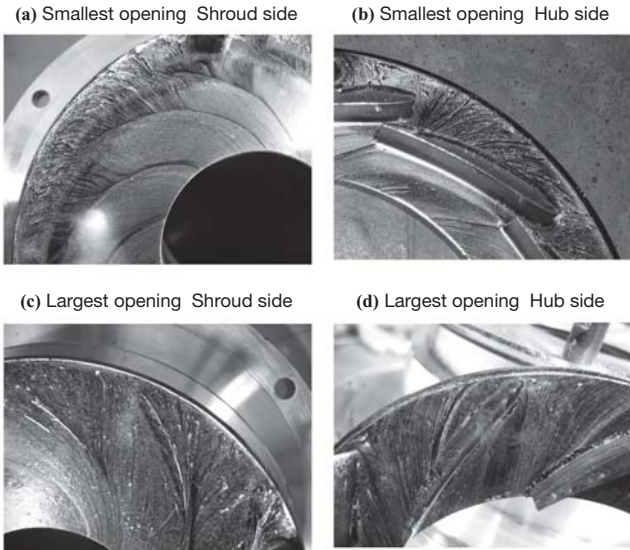


Fig. 6 Results of oil flow visualization

side is low over the entire nozzle vane, and the pressure on the pressure side is higher than on the suction side. Due to this pressure difference, the leakage flow of the clearance portion goes toward the suction side from the pressure side. This leakage flow spreads in the nozzle while forming a tip leakage vortex due to the pressure gradient from the outer radius to the inner radius of the nozzle. Visualization confirms that the tip leakage flow discharging from the pressure side to the suction side on the shroud wall side with clearance rolls up in the main flow and converges into the tip leakage vortex. On the other hand, the flow on the hub side without clearance smoothly increases in velocity.

In case of the largest opening (Fig. 5), the flow has a negative incidence against the nozzle, and the pressure on the suction side of the nozzle is higher than on the pressure side. On the pressure side, development of a low-speed area is observed due to the effect of the negative incidence, and at the latter half portion, the difference

in pressure between the suction side and pressure side decreases. The leakage flow passing the clearance due to the pressure difference between the suction side and pressure side goes to the pressure side from the suction side. This leakage flow is restrained to the pressure side due to the pressure gradient toward the inner radius from the outer radius of the nozzle and flows out while forming a tip leakage vortex along the nozzle pressure surface. Visualization reveals that the vane shape appears on the shroud wall side with a clearance. The reason is considered to be that the leakage flow is limited on the edge of the nozzle vane. In case of the largest opening, it is predicted that the effect of the leakage vortex on the flow field on the nozzle is limited. On the hub side, separation occurs on the pressure side. This separation reaches between the nozzle vanes.

The flow has a positive incidence for the smallest opening and negative incidence for the largest opening. Then the vane was rotated around the pivot, and the flow field where the incidence becomes 0 degree through the CFD (Computational Fluid Dynamics) was investigated. Figure 7 shows the calculation result when the incidence is 0 degree. The nozzle clearance is 0.75 mm only at the shroud side similar to the smallest and largest opening. When the incidence is 0, the low-speed area that appeared on the suction side of the largest opening is not observed. The pressure is almost equal between the pressure side and suction side, and the leakage flow goes from the pressure side to the suction side. Compared with the smallest opening, the pressure difference between the pressure side and suction side is small and the pressure gradient from the outer radius toward the inner radius is small, and so the amount of leakage is small and the leakage flow does not spread in the downstream of the vane.

Figure 8 shows the test results of the smallest opening. It shows the flow angle (measured from radial direction) and radial velocity C_r (inward flow is negative). θ indicates measuring position in the circumferential direction. The horizontal axis shows the spanwise position, 1.0 for the shroud side and 0.0 for the hub side. For the flow field measured, the flow angle is

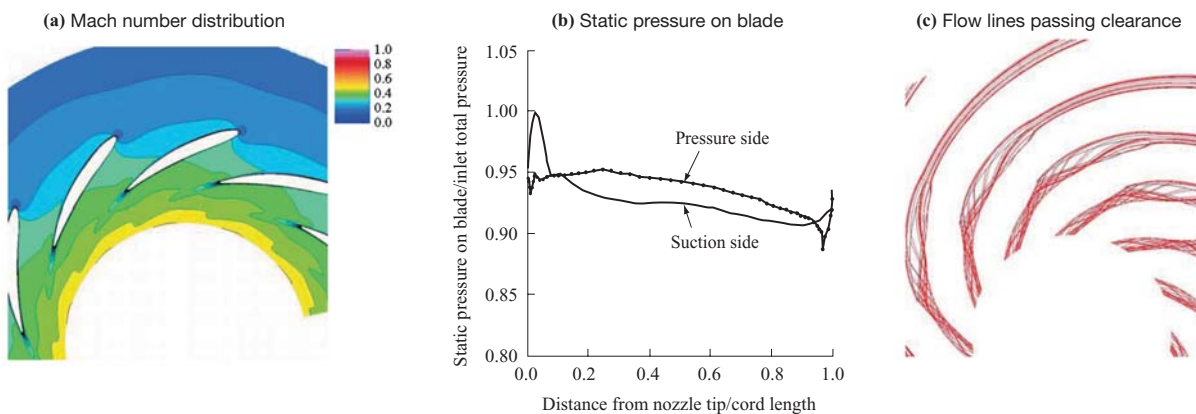


Fig. 7 Calculated result (Incidence angle = 0°)

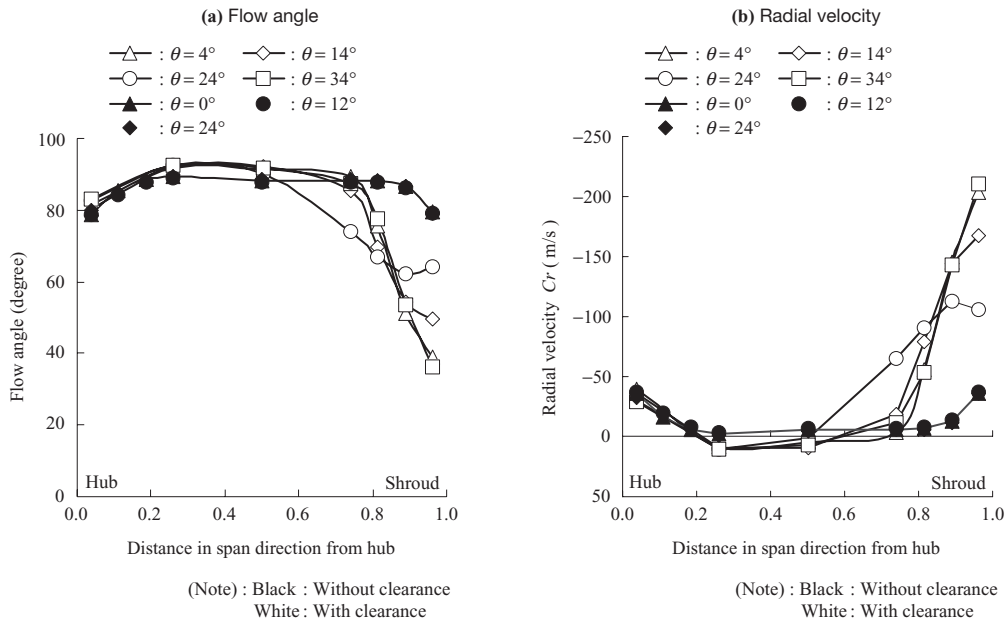


Fig. 8 Measurement result (Smallest opening)

small near the wall (radial velocity is high) and the flow angle at the mid-span portion is large (radial velocity is low). **Figure 9** shows the flow angle and radial velocity obtained by circumferentially mass averaging the results of CFD analysis and measurement. These are the results of measurement and analysis of the nozzle with the clearance. As both results agree qualitatively, it can be considered that the measurement and CFD analysis results capture the feature of the flow field to some extent. The velocity distribution shown in **Fig. 9** is considered to be formed as follows.

In case of the smallest opening, the main flow is turned in the circumferential direction by the nozzle, and the flow field with high circumferential velocity is formed. In this flow field, a pressure gradient occurs

from the outer radius to the inner radius as to balance with the centrifugal force due to the high circumferential velocity. Since the circumferential velocity within the boundary layer is smaller than that in the main flow, the flow in the boundary layer is turned in the radial direction by this pressure gradient. For this reason, the flow angle decreases near the wall and the radial velocity near the wall increases. As a result, the flow passing near the mid-span decreases and the area decreases toward the downstream, but near the mid-span the velocity component in the radial direction decreases. If the clearance exists, the flow passing through the clearance is not restricted by the nozzle vane, and so the flow angle near the wall surface on the side with the clearance (shroud side) further decreases and the velocity

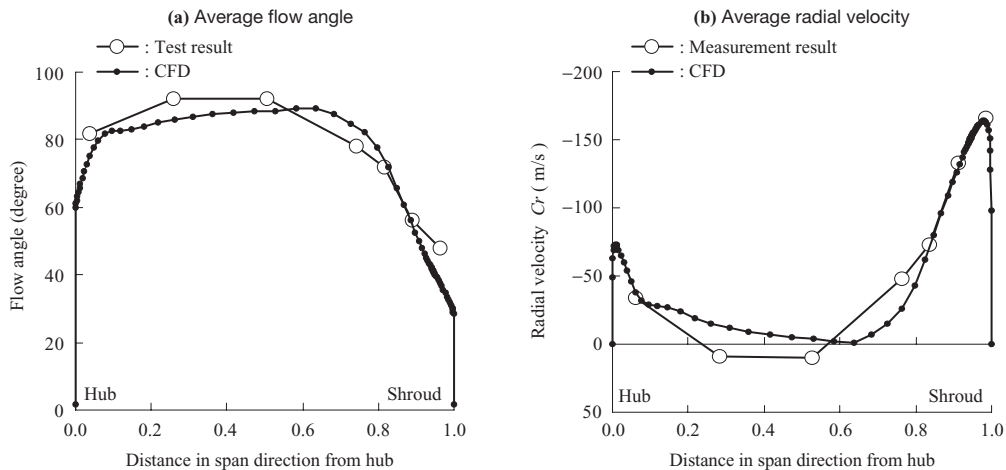


Fig. 9 Comparison of CFD with measurement (Smallest opening)

component in the radial direction increases.

Figure 10 shows the flow angle and radial velocity at each radial position that were obtained through the CFD analysis. These are analytical results when the clearance exists. As described above, it can be confirmed that as the radius decreases (approaching the measuring position), the radial velocity of the main flow decreases. **Figure 11** shows the flow angle and total pressure distribution on the cross section of the measuring position when the clearance exists. The outer frame of the figure shows for 2 pitches of nozzle horizontally, and the upper part is for the shroud and the lower part for the hub. On the

shroud side with clearance, the effect of leakage flow appears in the entire pitch direction. On the shroud side, a low total pressure area surrounded by the concentric curves exists. It is considered that this area is generated by the tip leakage vortex. The wake shedding from the nozzle trailing edge to the downstream of the vane tends to diffuse because the flow angle is large and the fluid path becomes long. **Figure 12** shows the total pressure distribution at the nozzle trailing edge **-(a)**, 2 mm **-(b)** and 4 mm **-(c)** downstream from the trailing edge, and measuring position (12.8 mm downstream) **-(d)**. It can be seen that the wake diffuses near the nozzle trailing

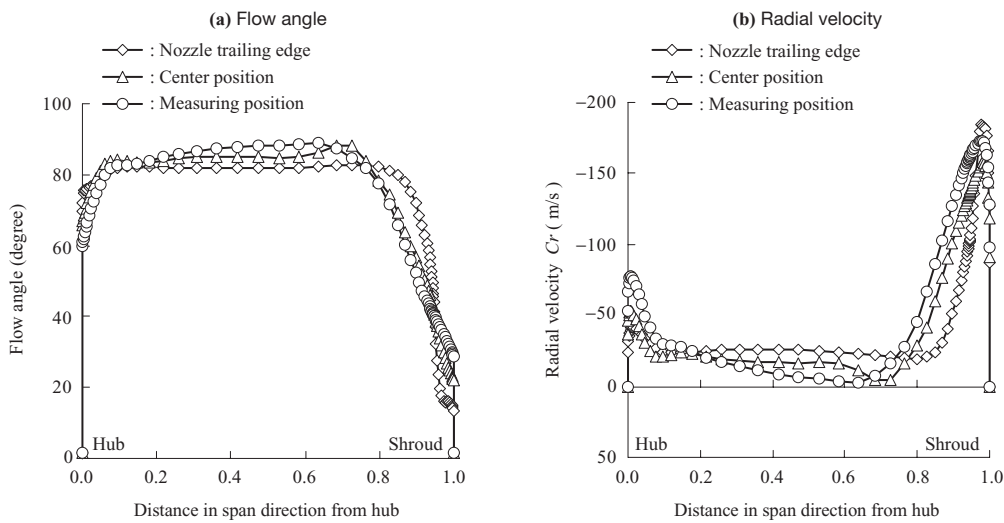


Fig. 10 Computed flow angle and radial velocity at different positions (Smallest opening)

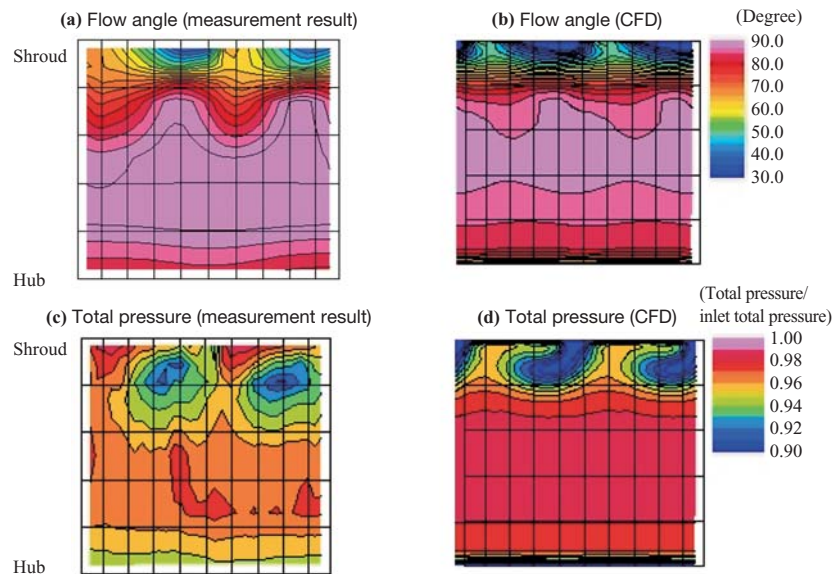
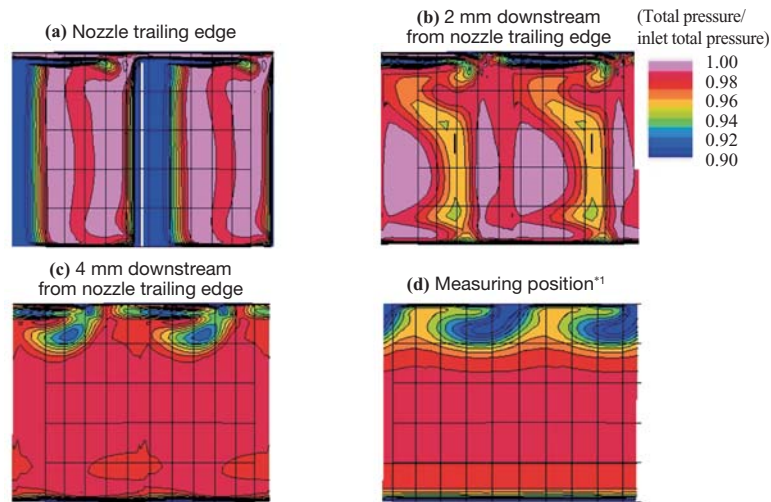


Fig. 11 Flow angle and total pressure distribution (Smallest opening)



(Note)*1 : 12.8 mm downstream from nozzle trailing edge

Fig. 12 Stagnation pressure downstream of nozzle trailing edge

edge and the effect of the leakage vortex soon becomes dominant.

Figure 13 shows the average flow angle of the largest opening -(a) and average radial velocity -(b). These are measurement and analysis results when the clearance exists. The results of CFD capture the characteristics of the measurement results, confirming that the measurement results and the CFD analysis are useful when discussing the flow field in the nozzle. Figure 14 shows the flow angle -(a) and radial velocity -(b) at each radial position that were obtained through the CFD analysis when assuming the clearance exists. The radial velocity increases as the radius decreases. Figure 15 shows the flow angle on the cross section of measuring position and total pressure distribution when the clearance exists. Since the area where the angle change occurs is almost the same on the hub side and shroud side, it can be judged that the effect of leakage flow on the flow field

is small. In the total pressure distribution, a band-like low total pressure area exists from the hub to the shroud. In case of the largest opening, the measuring position is adjacent to the nozzle trailing edge and the flow angle is much smaller compared with the smallest opening, and hence it is considered that the strong effect of the wake appears.

When the leakage flow was calculated from the results of CFD assuming that the flow crossing the centerline of the nozzle vane was the leakage flow, it was 31% of the total flow for the smallest opening and 5.6% for the largest opening. When the incidence was 0, it was 5.1%. If both hub and shroud sides were provided with clearance as in the case of actual nozzle and their values were assumed to be equivalent to those of the normal variable area nozzle, the recalculated leakage flow was 13.8% for the smallest opening and 1.3% for the largest opening. The leakage flow also shows that the smaller the nozzle

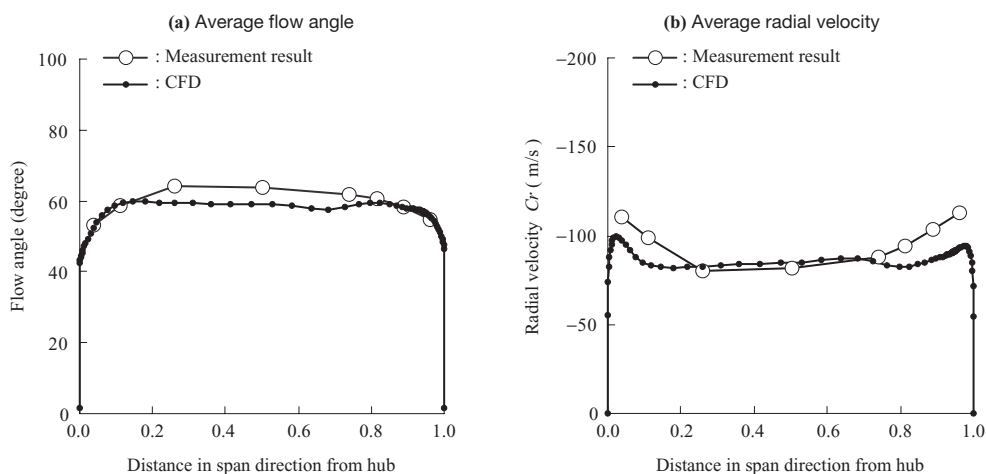


Fig. 13 Comparison of CFD with measurement (Largest opening)

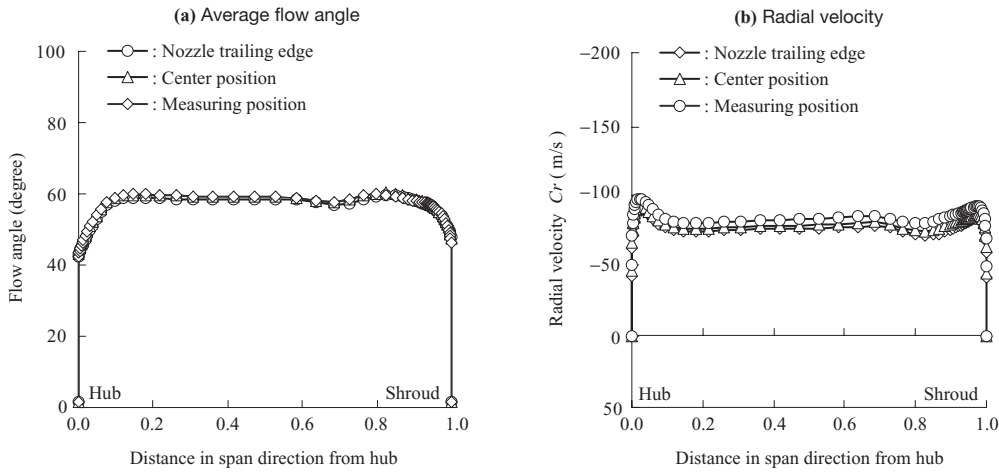


Fig. 14 Computed flow angle and radial velocity at different positions (Largest opening)

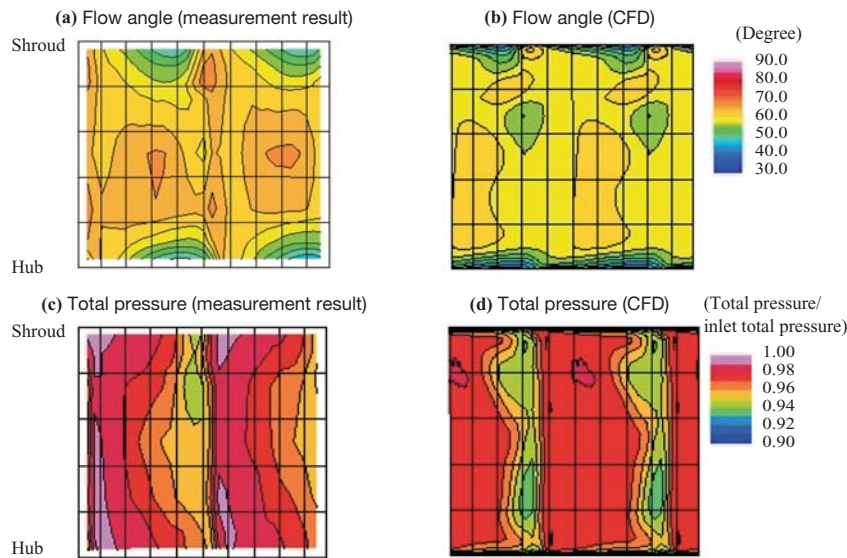


Fig. 15 Flow angle and total pressure distribution (Largest opening)

opening, the larger the effect of the leakage flow.

4. Conclusion

The flow field downstream of the variable area nozzle for radial turbine was investigated and the following results were obtained.

- (1) In case of the smallest opening of nozzle, the effect of the leakage flow becomes dominant in the flow field. Due to leakage vortex produced, distribution occurs with total pressure and flow angle in the entire pitch direction near the wall. The region where the lowest total pressure and flow angle appear is assumed to be the center of the tip leakage vortex.
- (2) In case of the largest opening of nozzle, the effect of the leakage flow on the flow field is small. In the

pitch direction, there exists a low pressure area that is considered to be caused by wake. It is a flow field where the effect of wake is dominant.

- (3) The existence of the nozzle clearance is a factor in decreasing a turbocharger performance during the period of the engine acceleration. When the engine is accelerated, it is necessary to increase a circumferential velocity and hence, to increase the nozzle setting angle. However, the increase of the leakage flow due to the large setting angle prevents a circumferential velocity from increasing and deteriorates the accelerating performance of the engine. It is, therefore, important to minimize the leakage flow at the largest setting angle in the design of the variable area nozzle system.

REFERENCES

- (1) P. L. Meitner and A. J. Glassman : Loss Model for Off-Design Performance Analysis of Radial Turbines With Pivoting-Vane Variable-Area, SAE Technical Papers 801135 (1980.10) pp. 1-12
- (2) F. Faibanks : The Determination of Deviation Angles at Exit from the Nozzle of Inward Flow Radial Turbine, ASME paper 80-GT-147 (1980.3) pp. 1-7
- (3) Y. Okazaki, N. Matsudaira, et al. : A case of variable geometry turbocharger development, C111/86 IMechE (1986) pp. 191-195
- (4) K. Matsumoto, Y. Jinnai, et al. : Development of variable geometry turbocharger for diesel passenger car, C554/005/98 IMechE (1998.11) pp. 329-346
- (5) H. Hayami, Y. Hyun, et al. : Flow field in outlet of variable nozzle for radial turbine, The Report of the Research Institute of Industrial Science, Kyushu University Report No. 82 (1987. 3) pp. 149-158
- (6) Y. Senoo, M. Yamaguchi, Y. Hyun and H. Hayami : The influence of tip-clearance on the performance of nozzle blades radial turbines, JSME International Journal Vol. 30 No. 264 (1987) pp. 929-935
- (7) Y. Hyun, Y. Senoo, M. Yamaguchi and H. Hayami : The influence of tip clearance on the performance of nozzle blades radial turbines (Experimental and performance prediction at three nozzle angles), JSME International Journal Series 2 Vol.31 No.2 (1988) pp. 258-262